Food Chemistry: X 39 (2026) 104405

Contents lists available at ScienceDirect

Food Chemistry: X

journal homepage: www.sciencedirect.com/journal/food-chemistry-x

Analytical Methods

Insights into differences in oxidation and interaction of main components in porcine and bovine milk during refrigerated storage

Qiao Jiang [a,1], Haixia Yan [b,1], Mo Li [c], Li Zhou [a], Jie Wu [a,d,*], Xin Zhao [a,d,*]

[a] School of Public Health, Shenyang Medical College, North Huanghe Street No.146, Shenyang 110034, China
[b] School of Biological Science and Biotechnology, Minnan Normal University, No. 36 Xianqian Zhijie, Zhangzhou, 363000, China
[c] College of Criminal Science and Technology, Criminal Investigation Police University of China, Tawan Street No. 83, Shenyang 110031, China
[d] Liaoning Medical Functional Food Professional Technology Innovation Center, Shenyang Medical College, Shenyang, Liaoning 110034, China

ARTICLE INFO

Keywords:
Porcine milk
Refrigerated storage
Oxidation pathways
OPLS-DA

ABSTRACT

Oxidation and interactions of components in porcine milk (PM) and bovine milk (BM) during 6-day storage at 4 °C were investigated. Compared to BM, PM exhibited higher levels of lipid oxidation products, protein carbonyl and surface hydrophobicity ($P < 0.05$), with protein aggregation, indicating PM underwent more extensive lipid and protein oxidation. In contrast, BM showed higher 3-deoxyglucosone (3-DG) and D-glucosone (GLO) accumulation, greater sulfhydryl loss, enhanced fluorescence, and fluctuating particle size, suggesting carbohydrate oxidation and glycation reaction. Orthogonal projection to latent structures discriminant analysis identified surface hydrophobicity, thiobarbituric acid-reactive substances (TBARS), particle size and sulfhydryl groups as discriminators of PM and BM oxidation states. TBARS in PM correlated with particle size, carbonyl and sulfhydryl groups ($P < 0.05$), whereas BM surface hydrophobicity correlated with 3-DG and GLO contents ($P < 0.05$). Thus, lipid oxidation in PM was associated with protein changes, whereas in BM such changes paralleled glycation driven by carbohydrate oxidation and glycation reaction.

1. Introduction

Bovine milk (BM) is rich in proteins, lipids, carbohydrates, various minerals and vitamins, making it highly nutritious. Currently, BM is the main milk source for infant formula worldwide (Qin et al., 2022; Zhang et al., 2022). However, in many countries, raw milk cannot be processed immediately after milking and usually has an additional storage period (Li et al., 2022). During storage, complex chemical reactions occurred among the main nutritional components in raw milk such as lipids, protein and carbohydrates. This was the primary reason for the deterioration of functional properties, decline of nutritional value, formation of unpleasant flavors and even the generation of harmful substances (Li et al., 2022; Malacarne et al., 2013).

During the storage of raw milk, carbohydrate oxidation, glycation reactions or lipids can produce reactive α-dicarbonyl compounds (such as glyoxal: GO, methylglyoxal: MGO, D-glucosone: GLO, 3-deoxyglucosone: 3-DG etc.), which are highly reactive towards nucleophilic groups (such as lysine, arginine and other residues) (Akıllıoğlu, Chatterton, & Lund, 2022). Meanwhile, lipid oxidation products (such as acrolein, malondialdehyde, etc.) can also interact with the above nucleophilic amino acid residues, further leading to changes in spatial conformation of protein, inactivation of functional groups, and even protein aggregation (Milkovska-Stamenova, Mnatsakanyan, & Hoffmann, 2017). Furthermore, these α-dicarbonyl compounds can react with proteins, forming advanced glycation end products (AGEs), such as N^{ε}-(carboxymethyl)lysine, N^{ε}-(carboxyethyl)lysine, pyrraline, etc. (Dong et al., 2023). Under refrigerated storage conditions, protein denaturation, aggregation, and cross-linking also occur, which may alter the structure of protein (Ye et al., 2022). Due to the formation of AGEs and the generation of cross-linked substances, the changes in protein structure will result in the reduction in nutritional components. Therefore, it is crucial to elucidate the chemical changes in raw milk components during storage.

At present, researching the stability of raw milk during storage mainly focuses on common large mammalian milk sources such as BM, sheep milk and camel milk (Li et al., 2022), while there are few systematic studies on porcine milk (PM). PM has received widespread attention for its unique nutritional composition, its protein and lipid

* Corresponding author at: School of Public Health, Shenyang Medical College, North Huanghe Street No.146, Shenyang 110034, China.
E-mail address: zhaoxin@symc.edu.cn (X. Zhao).
[1] Equivalent contributions.

https://doi.org/10.1016/j.fochx.2026.104405
Received 15 June 2026; Received in revised form 26 August 2026; Accepted 1 September 2026
Available online 4 September 2026
2590-1575/© 2026 The Authors. Published by Elsevier Ltd. This is an open access article under the CC BY-NC-ND license (http://creativecommons.org/licenses/by-nc-nd/4.0/).

contents significantly higher than those of human milk and BM. Moreover, compared with other domesticated animal milk, oligosaccharide content of PM is closer to that of human milk (Zhao et al., 2024; Zhao, Cao, Quan, Liu, & Yue, 2025). In recent years, studies on raw BM during storage has laid a foundation for understanding changes in its main components, physicochemical properties, and processing characteristics (Li et al., 2022; Malacarne et al., 2013). Although these studies have provided important references for analyzing the changes in component stability during the storage of raw milk, there are significant differences in nutritional characteristics between PM and BM. Therefore, research on the storage of PM remains essential. In particular, a systematic comparison between PM and BM from the perspective of main component interactions has yet to be conducted. In this context, investigating the main component changes and their interactions during the storage of PM is of great significance for promoting its application as a high-value milk source. Therefore, this study was designed to compare the main components and explore the potential mechanisms underlying the differential oxidation and interaction patterns in PM and BM collected from conventional commercial farms during refrigerated storage. For this purpose, PM and BM samples were stored at 4 °C for 6 days and the changes in protein structure, lipid oxidation, and glycation level were monitored. The research findings not only serve as a foundation for the further exploitation of PM, but also are of great significance to the development of the dairy industry.

2. Materials and methods

2.1. Materials

All PM was collected from a certain pig farm in Shenyang City, and all BM was collected from a certain modern ranch in Shenyang City. The feeding environment and conditions of all the lactating porcines and cattles in the experiments were consistent within each group. The diets were formulated according to the nutritional requirements of each species and thus were not standardized across species. Mature milk samples were collected from PM (15–20 days, $n = 40$) and BM ($n = 40$). To ensure sample representativeness, pooled milk samples were obtained from all individuals within each group (Jin et al., 2026; Ratel et al., 2024). After being immediately cooled on dry ice, the milk samples were returned to laboratory. GO (40%) and MGO (40%) were supplied by Shanghai Macklin Biochemical Technology Co., Ltd. (Shanghai, China). Methanol (99%) was obtained from Sigma-Aldrich (St Louis, MO, USA). 3-DG (95%) and GLO (95%) standards were provided by Toronto Research Chemicals, Inc. (Toronto, ON, Canada). All other reagents were obtained in the highest purity available.

2.2. Preparation of sample

Raw milk samples from PM and BM were pooled separately before the experiment to minimize individual variation. A 310 mL aliquot was taken from each pooled sample. These aliquots were stored at 4 °C for 6 days, during which they were sampled at 1-day intervals. After collection, samples were preserved at −80 °C until further detection. These samples were named according to group and sampling time (e.g., PM_0, BM_0 for the initial time point). All samples were analyzed in triplicate.

2.3. Determination of raw milk composition

The levels of protein, lipids, lactose and other components of PM and BM were analyzed with a milk analyzer (FOSS, Hillerød, Denmark), and each sample was tested three times.

2.4. Determination of lipid oxidation

2.4.1. Peroxide value (POV)

Samples were assayed for the POV values using the method of Yan et al. (2024). Sample aliquots were combined with methanol and chloroform in a 1:1:2 volume ratio. After centrifugation (8000 rpm, 10 min), the supernatant (1 mL) was diluted 1:9 (v/v) with methanol-chloroform (7:3, v/v) and shaken. 50 μL each of ferrous chloride (3.5 g/L) and ammonium thiocyanate solution (300 g/L) were added. After dark incubation (25 °C, 5 min), absorbance at 500 nm was recorded. A standard curve was established using cumene hydroperoxide, based on which the lipid peroxidation content was calculated via Eq.(1) and expressed as μmol cumene hydroperoxide/mL milk.

$$\text{POV content} = (C \times V1 \times n)/V2 \quad (1)$$

where C (μmol/L) is the peroxide concentration calculated by standard curve; V_1 (mL) and V_2 (mL) are the sample volumes of the color reaction and the sample, respectively; n is dilution factor.

2.4.2. Thiobarbituric acid-reactive substances (TBARS)

Samples were assayed for the TBARS values following the described by Yan, Huang, et al. (2024). Samples were mixed with trichloroacetic acid (7.5%) at a 1:1 volume ratio. After centrifuge (8000 rpm, 15 min), supernatant was mixed with thiobarbituric acid-acetic acid solution (20 mmol/L) at a 1:1 volume ratio. Then the mixtures were heated in a boiling water bath for 40 min and immediately cooled on ice. The absorbance was measured at 532 nm. TBARS concentration was calculated via Eq.(2) using a standard curve of 1,1,3,3-tetramethoxypropane and expressed as μmol malonaldehyde/mL milk.

$$\text{TBARS content} = (C \times n)/V \quad (2)$$

where C (μmol/L) is the malondialdehyde concentration obtained from the standard curve; V (mL) is sample volume; n is dilution factor.

2.5. Determination of the amino acid (AA) contents

The 400 μL samples and 3.6 mL of 6 mol/L HCl (containing 0.01% phenol) were mixed, and hydrolyze at 100 °C for 24 h. The hydrolysates were diluted twice and filtered through 0.22 μm filters. After N_2 evaporation of 200 μL of the filtered samples to dryness, the residue was reconstituted to 1 mL with sodium citrate buffer (pH 2.2), then re-filtered prior to testing.

AA contents of raw milk were determined using the L-8900 fully automatic AA analyzer (Hitachi, Japan). The column temperature of the instrument and reaction were 57.0 °C and 135 °C, the flow rate of pump I and pump II were 0.45 mL/min and 0.35 mL/min, with an injection volume of 20 μL. Absorbance of proline was measured at 440 nm, and other AA were recorded at 570 nm. The AA contents were based on the standard AA contents using Eq.(3):

$$C1 = (A1 \times C2 \times n)/A2 \quad (3)$$

where C_1 (mmol/L) and C_2 (mmol/L) are each AA concentration in samples and standards, respectively;, A_1 and A_2 are each AA peak area in samples and standards, respectively; n is dilution factor.

2.6. Determination of carbonyl groups

Carbonyl groups ware determined according to Yan, Ma, Shen, Ye, and Liu (2024) with slight modifications. 0.5 mL samples (diluted 20 times) and 0.5 mL of 2 mol/L HCl (containing 10 mmol/L 2,4-dinitrophenylhydrazine, DNPH) were mixed and kept at 25 °C in dark for 1 h. After adding 0.5 mL trichloroacetic acid (40%) and mixing well, the mixtures were incubated for 10 min. Centrifugation for 10 min (10,000 rpm), the precipitates were dissolved in 0.6 mL guanidine hydrochloride (6 mol/L) and kept at 37 °C for 15 min. After centrifugation (10,000 rpm, 3 min), the absorbance of samples was measured at 370 nm, and the carbonyl contents were calculated with a molar refractive index of 22,000, expressed as nmol DNPH/mg of protein. The sample without

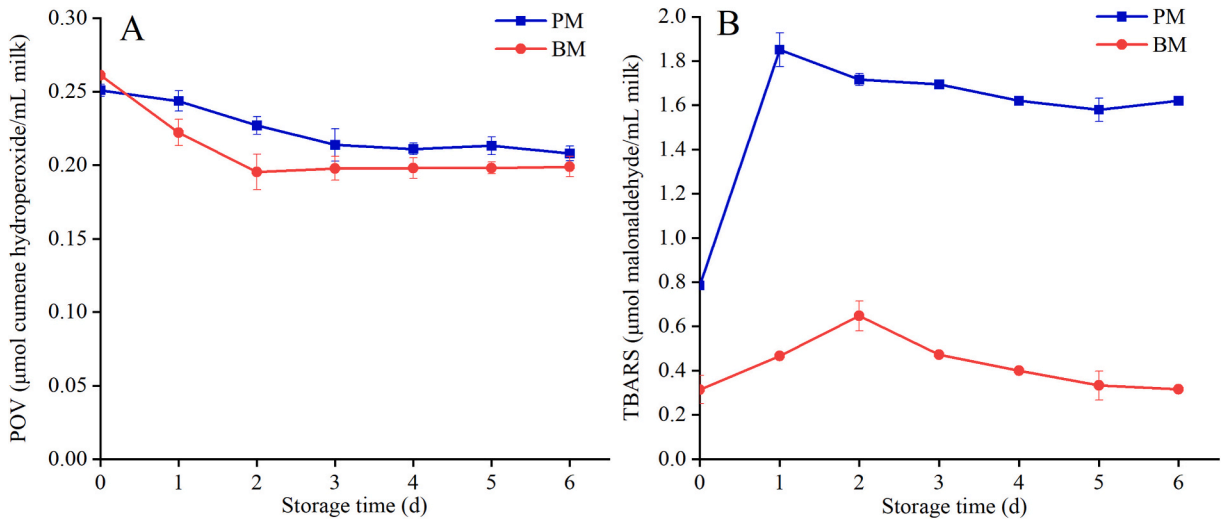


Fig. 1. POV (A) and TBARS (B) of BM and PM at 4 °C for 6 days.

2,4-dinitrophenylhydrazine was the blank control. The concentrations of carbonyl groups were calculated using Eq. (4):

$$X = (45.45 \times A \times n)/C \quad (4)$$

where X (nmol/mg protein) is carbonyl group concentration; A is absorbance of sample; C is protein concentration in samples; n is dilution factor.

2.7. Determination of sulfhydryl groups

Sulfhydryl groups of samples were quantified as described by He, Wang, Wang, and Ji (2026). Samples and methanol were mixed at a 1:1 volume ratio, and centrifuged (10,000 rpm,10 min) to remove proteins and lipids. Then 0.5 mL samples, 5 mL Tris-Gly buffer and 20 μL Ellman reagent were incubated at 25 °C for 15 min in dark. After centrifugation (8000 rpm, 10 min), the sample absorbance at 412 nm was recorded, using a solution without DTNB as blank. The sulfhydryl group concentrations were calculated using Eq. (5):

$$X = 73.53 \times A \times n/C \quad (5)$$

where X (μmol/g protein) is sulfhydryl group concentration; A is the absorbance of samples, C (mg/mL) is the protein concentration in samples; n is dilution factor.

2.8. Determination of surface hydrophobicity

Surface hydrophobicity was measured following a previously reported method (Han, Wang, Wang, & Tang, 2020). The protein content in samples was diluted to 0.01, 0.05, 0.1, 0.5, and 1 mg/mL, respectively. The diluted samples (4 mL) were combined with 20 μL of 8 mmol/L 8-Anilino-1-naphthalenesulfonic acid solution (in 50 mmol/L phosphate buffer, pH 7.4), and incubated at 25 °C in dark for 1 h. Measurements were performed at excitation and emission wavelengths of 390 nm and 470 nm, respectively. Surface hydrophobicity (H_0) of protein sample was determined as the slope (k) obtained from plotting fluorescence intensity against protein content.

2.9. Determination of endogenous fluorescence

The samples were diluted with phosphate buffer (0.01 mol/mL, pH 7.0) to reach a final protein level of 0.1 mg/mL, then scanned using a Hitachi FL-4600 fluorometer (Tokyo, Japan) using a 10 nm slit.

2.10. Determination of particle size

A 1:1000 dilution of samples was performed, and the particle sizes were measured with a particle size and zeta potential analyzer (Zetasizer nano, Malvern, Worcestershire, U.K.).

2.11. Sodium dodecyl sulfatepolyacrylamide gel electrophoresis (SDS-PAGE)

Following the method previously presented by Yan, Ma, et al. (2024). Protein content of samples was adjusted to 2 mg/mL and then combined with an equal volume (1:1 v/v) of protein loading buffer. The mixture was heated in a boiling water for 5 min to ensure complete protein denaturation. Aliquots of 10 μL were subsequently applied to the gel. Following electrophoresis, the gel was incubated with coomassie brilliant blue R250 for 30 min and decolorized until the bands become clear. Finally, the gel was imaged using an GE AI600UV imager (GE Healthcare, Boston, MA, America).

2.12. Determination of α-carbonyl compounds

According the method of Zhao et al. (2021) with some modifications. The 200 μL of samples and 400 μL methanol were mixed by vortexing. After centrifugation (10,000 rpm, 10 min), 100 μL supernatant aliquot was diluted 5 times, mixed with 0.5 mL OPD solution (20 mg/mL), and derivatized at 4 °C for 12 h, then filtered through 0.22 μm filter. Standard samples were derivatized and diluted in the same way, and a series of standard solutions was intended to ploted the standard curve. The α-carbonyl compound contents were qualified using an ultra performance liquid chromatography-tandem mass spectrometry (Waters Technologies Co., Ltd., Milford, MA, USA) with a reversed-phase C_{18} column (2.1 mm × 15 mm, 3 μm, Welch Materials, Inc.). Methanol and 0.1% formic acid in water (70:30) served as the mobile phase, with isocratic elution. Flow rate and injection volume were 0.20 mL/min and 2 μL, respectively. Carbonyl compounds were quantified using the following procedure: GO, *m/z* 131 → 77; MGO, *m/z* 145 → 77; 3-DG, *m/z* 235 → 199; GLO, *m/z* 251 → 173. Data acquisition and quantitative processing were performed using MassLynx software (Version 4.2, Waters Corp., USA). Carbonyl levels were determined using standard curves, and all curves showed correlation coefficient (R^2) values>0.999. The limits of detection (LOD) and quantification (LOQ) were determined by the signal-to-noise approach, defined at those levels resulting in signal-to-noise ratios of 3:1 and 10:1, respectively (Meucci et al., 2025). The detailed values were provided in Supplementary Table S1.

Table 1
AA content (mmol/L) change of PM during storage.[a]

	Rt	0	1	2	3	4	5	6
Asp	5.40	38.21 ± 1.34^{b}	35.44 ± 0.31^{f}	36.18 ± 0.08^{d}	35.77 ± 1.51^{e}	36.50 ± 1.03^{c}	39.60 ± 0.94^{a}	35.42 ± 0.35^{f}
Thr	6.12	23.31 ± 0.75^{b}	20.93 ± 0.33^{f}	21.47 ± 0.07^{d}	21.24 ± 0.30^{e}	21.77 ± 0.66^{c}	24.04 ± 0.41^{a}	20.81 ± 0.44^{g}
Ser	6.82	24.19 ± 0.80^{b}	22.57 ± 0.57^{f}	22.98 ± 0.46^{d}	22.73 ± 0.95^{e}	23.32 ± 1.18^{c}	25.15 ± 0.86^{a}	20.59 ± 0.32^{g}
Glu	7.54	120.99 ± .85^{b}	113.36 ± .19^{f}	115.45 ± .15^{d}	114.25 ± .19^{e}	116.29 ± .40^{c}	126.58 ± .74^{a}	112.05 ± .59^{g}
Pro	8.77	62.70 ± 0.89^{f}	56.53 ± 0.68^{h}	58.85 ± 0.31^{g}	87.45 ± 3.07^{b}	88.27 ± 1.23^{a}	66.41 ± 0.12^{e}	84.56 ± 1.64^{c}
Gly	10.97	15.57 ± 0.44^{b}	14.64 ± 0.44^{f}	15.00 ± 0.10^{d}	14.83 ± 0.85^{e}	15.10 ± 0.53^{c}	16.30 ± 0.46^{a}	14.70 ± 0.31^{f}
Ala	11.62	9.65 ± 0.57^{b}	8.88 ± 0.42^{d}	8.83 ± 0.28^{e}	8.75 ± 0.41^{f}	9.04 ± 0.31^{c}	9.80 ± 0.45^{a}	8.13 ± 0.68^{g}
Cys	11.98	5.25 ± 0.06^{b}	4.87 ± 0.66^{c}	4.53 ± 0.72^{e}	4.60 ± 0.47^{d}	3.81 ± 0.08^{g}	4.40 ± 0.05^{f}	5.75 ± 0.54^{a}
Val	12.59	23.95 ± 1.04^{b}	22.48 ± 0.69^{g}	22.95 ± 0.23^{d}	22.52 ± 1.18^{f}	23.01 ± 0.70^{c}	25.05 ± 0.67^{a}	22.62 ± 0.33^{e}
Met	13.74	6.04 ± 0.27^{b}	5.77 ± 0.24^{e}	5.65 ± 0.16^{g}	5.79 ± 0.33^{d}	5.93 ± 0.25^{c}	6.40 ± 0.23^{a}	5.67 ± 0.13^{f}
Ile	16.03	18.12 ± 0.74^{b}	17.00 ± 0.58^{f}	17.32 ± 0.17^{c}	16.94 ± 0.94^{g}	17.30 ± 0.60^{d}	18.84 ± 0.46^{a}	17.09 ± 0.47^{e}
Leu	17.16	49.80 ± 0.41^{b}	45.57 ± 1.51^{f}	46.43 ± 0.48^{d}	45.63 ± 2.88^{e}	46.47 ± 1.63^{c}	50.50 ± 1.60^{a}	45.33 ± 1.15^{g}
Tyr	18.07	8.45 ± 0.44^{b}	7.98 ± 0.35^{f}	8.14 ± 0.17^{c}	7.96 ± 0.61^{g}	8.11 ± 0.41^{d}	8.79 ± 0.35^{a}	8.01 ± 0.26^{e}
Phe	18.97	17.24 ± 0.86^{b}	16.13 ± 0.67^{f}	16.42 ± 0.23^{d}	16.21 ± 0.97^{e}	16.50 ± 0.51^{c}	17.93 ± 0.50^{a}	16.22 ± 0.62^{e}
Lys	21.31	26.30 ± 1.04^{b}	24.14 ± 0.06^{g}	25.07 ± 0.05^{d}	24.81 ± 1.32^{e}	25.37 ± 0.86^{c}	27.48 ± 0.70^{a}	24.76 ± 0.57^{f}
His	26.05	9.62 ± 0.55^{b}	9.06 ± 0.56^{f}	9.30 ± 0.55^{c}	9.12 ± 0.88^{e}	9.15 ± 0.61^{d}	10.03 ± 0.58^{a}	9.03 ± 0.43^{g}
Arg	27.58	15.83 ± 0.47^{b}	14.68 ± 0.37^{g}	15.09 ± 0.13^{d}	14.83 ± 0.44^{f}	15.21 ± 0.01^{c}	16.00 ± 0.74^{a}	15.00 ± 0.22^{e}
TAA		463.80 ± 30.27^{e}	440.06 ± 7.17^{g}	449.66 ± 3.14^{f}	473.42 ± 16.13^{c}	481.14 ± 53.98^{b}	493.29 ± 10.39^{a}	465.74 ± 3.92^{d}

Thr, threonine; Val, valine; Met, methionine; Ile, isoleucine; Leu, leucine; Phe, phenylalanine; Lys, lysine; His, histidine; Asp, aspartic acid; Ser, serine; Glu, glutamic acid; Gly, glycine; Ala, alanine; Cys, cysteine; Tyr, tyrosine; Arg, arginine; Pro, proline; TAA, total amino acids.

[a] Note: a-h represented the significance of the same group at different storage time.

2.13. Statistical analysis

Data were analyzed using SPSS 25.0 software (IBM Corp., Armonk, NY, USA). Statistical methods included one-way analysis of variance (ANOVA) followed by Duncan's multiple range test for post-hoc comparisons, Pearson correlation analysis, and *t*-test. All results were expressed as mean ± SD and $P < 0.05$ or 0.01 indicated different levels of correlation or significance. Simca-p 14.0 software (Umetrics AB, Umeå, Sweden) was used for orthogonal projection to latent structures discriminant analysis (OPLS-DA). OriginPro 2024 (OriginLab Corporation, Northampton, MA, USA) was performed for data visualization.

3. Results and discussion

3.1. Analysis of the degree of lipid oxidation

Lipids are the main macromolecules in milk and essential for providing essential fatty acids, phospholipids and fat-soluble vitamins (Ji et al., 2025). As lipid oxidation drives quality deterioration in milk and off-flavors have been linked to increased POV (Pont, 1952), POV monitoring serves as an essential indicator for evaluating the oxidative state of milk. The storage experiment was initiated immediately upon arrival, with samples collected on 0 d serving as the baseline. As depicted in Fig. 1A, the POV values in PM were significantly higher than those in BM ($P < 0.05$), attributting to species-specific differences in fatty acid composition (Mitina et al., 2020). PM contained a higher proportion of long-chain polyunsaturated fatty acids, whereas BM was richer in saturated fatty acids (Wu et al., 2023), rendering PM more susceptible to oxidation and thus leading to its higher POV. Lipid hydroperoxides are unstable primary oxidation products prone to decompose into secondary products (such as aldehydes and ketones) (Fernandez-Avila, Gutierrez-Merida, & Trujillo, 2017). Accordingly, the POV decreased in both PM and BM, and this downward trend suggests the progressive transformation of hydroperoxides during storage. The TBARS values serve as an indicator of secondary oxidation products generated during the oxidation of dairy products (Pont, 1952). Compared with BM, the TBARS values in PM were significantly higher ($P < 0.05$, In Fig. 1B), and the TBARS values in PM and BM reached their maximum values on 1 d and 2 d respectively and then decreased, indicating that the lipid oxidation process in PM was more advanced during

Table 2
AA content (mmol/L) change of BM during storage.[a]

	Rt	0	1	2	3	4	5	6
Asp	5.40	18.35 ± 0.37^{f}	20.99 ± 0.33^{b}	20.41 ± 1.91^{d}	16.15 ± 0.36^{h}	18.26 ± 0.22^{g}	20.62 ± 0.20^{c}	19.37 ± 0.04^{e}
Thr	6.12	11.71 ± 1.20^{g}	13.62 ± 0.69^{d}	14.05 ± 1.71^{b}	10.69 ± 0.73^{h}	12.25 ± 0.30^{f}	13.92 ± 0.26^{c}	13.13 ± 0.40^{e}
Ser	6.82	11.83 ± 1.85^{g}	14.26 ± 0.62^{c}	13.41 ± 0.13^{d}	10.81 ± 0.87^{h}	12.93 ± 0.12^{f}	14.58 ± 0.31^{b}	13.06 ± 0.60^{e}
Glu	7.54	55.30 ± 4.89^{f}	64.64 ± 0.87^{c}	36.82 ± 0.57^{h}	49.41 ± 2.29^{g}	57.27 ± 0.96^{e}	64.76 ± 1.02^{b}	59.37 ± 0.95^{d}
Pro	8.77	24.85 ± 1.34^{g}	29.30 ± 1.50^{d}	38.62 ± 0.12^{b}	23.69 ± 0.98^{h}	26.27 ± 0.07^{f}	45.53 ± 1.85^{a}	27.96 ± 1.02^{e}
Gly	10.97	5.11 ± 0.26^{h}	5.89 ± 0.02^{f}	6.09 ± 0.92^{d}	5.14 ± 0.74^{g}	5.89 ± 1.13^{e}	7.90 ± 2.63^{a}	6.25 ± 1.11^{b}
Ala	11.62	4.38 ± 0.34^{g}	5.59 ± 0.13^{c}	5.15 ± 0.14^{d}	4.30 ± 0.13^{h}	4.96 ± 0.42^{f}	5.69 ± 0.10^{b}	5.08 ± 0.02^{e}
Cys	11.98	0.39 ± 0.02^{h}	1.12 ± 0.20^{b}	0.73 ± 0.07^{f}	0.78 ± 0.00^{e}	0.70 ± 0.91^{g}	0.85 ± 0.81^{d}	1.04 ± 0.09^{c}
Val	12.59	14.29 ± 0.73^{f}	16.45 ± 0.02^{c}	15.26 ± 0.49^{d}	12.78 ± 0.47^{g}	14.67 ± 0.95^{e}	16.73 ± 0.53^{b}	15.25 ± 0.19^{d}
Met	13.74	3.80 ± 0.37^{f}	4.30 ± 0.12^{c}	4.00 ± 0.01^{d}	3.38 ± 0.02^{g}	3.88 ± 0.17^{e}	4.39 ± 0.01^{b}	4.01 ± 0.03^{d}
Ile	16.03	11.30 ± 0.65^{g}	12.89 ± 0.22^{c}	11.72 ± 0.28^{e}	9.87 ± 0.16^{h}	11.37 ± 0.44^{f}	13.06 ± 0.03^{b}	12.24 ± 0.21^{d}
Leu	17.16	25.95 ± 1.84^{g}	29.75 ± 0.57^{c}	27.21 ± 0.62^{e}	23.10 ± 0.49^{h}	26.49 ± 0.78^{f}	30.11 ± 0.03^{b}	28.07 ± 0.37^{d}
Tyr	18.07	4.45 ± 0.52^{g}	5.04 ± 0.34^{c}	4.67 ± 0.26^{f}	4.03 ± 0.09^{h}	4.74 ± 0.24^{e}	5.34 ± 0.08^{b}	4.99 ± 0.18^{d}
Phe	18.96	9.95 ± 0.03^{f}	11.40 ± 0.46^{b}	10.24 ± 0.26^{e}	8.57 ± 0.07^{h}	9.71 ± 0.33^{g}	11.00 ± 0.13^{c}	10.36 ± 0.27^{d}
Lys	21.31	13.21 ± 0.96^{g}	15.50 ± 0.04^{b}	14.09 ± 0.02^{e}	11.92 ± 0.12^{h}	13.55 ± 0.29^{f}	14.66 ± 1.06^{c}	14.23 ± 0.09^{d}
His	26.05	4.09 ± 0.85^{g}	4.80 ± 0.51^{d}	5.98 ± 1.95^{a}	3.86 ± 0.00^{h}	4.42 ± 0.17^{f}	5.08 ± 0.05^{c}	4.69 ± 0.24^{e}
Arg	27.58	5.94 ± 0.10^{f}	6.90 ± 0.46^{b}	6.19 ± 0.19^{d}	5.05 ± 0.03^{h}	5.74 ± 0.11^{g}	6.45 ± 0.04^{g}	6.10 ± 0.13^{e}
TAA		224.91 ± 16.07^{g}	262.45 ± 3.81^{c}	234.63 ± 5.52^{e}	203.52 ± 4.95^{h}	233.09 ± 7.01^{f}	280.65 ± 0.39^{a}	245.22 ± 0.30^{d}

Thr, threonine; Val, valine; Met, methionine; Ile, isoleucine; Leu, leucine; Phe, phenylalanine; Lys, lysine; His, histidine; Asp, aspartic acid; Ser, serine; Glu, glutamic acid; Gly, glycine; Ala, alanine; Cys, cysteine; Tyr, tyrosine; Arg, arginine; Pro, proline; TAA, total amino acids.

[a] Note: a-h represented the significance of the same group at different storage time.

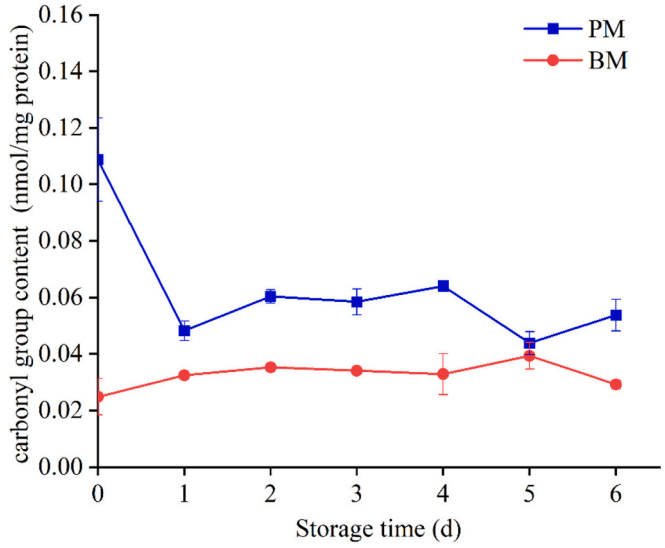


Fig. 2. Carbonyl group contents of BM and PM at 4 °C for 6 days.

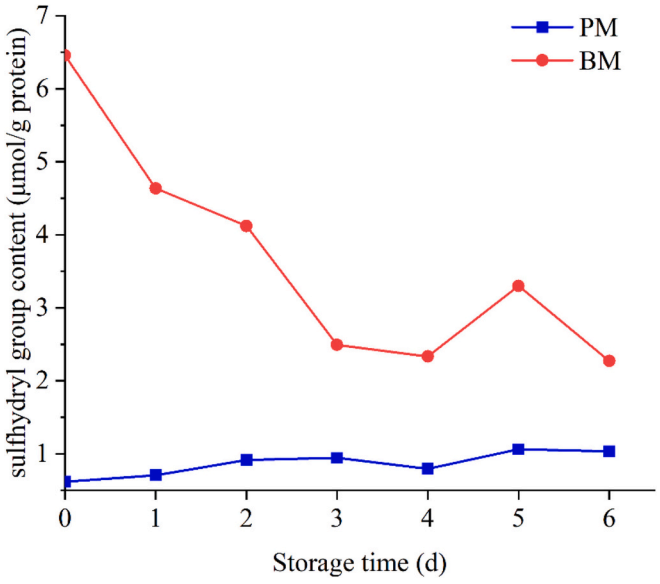


Fig. 3. Sulfhydryl group contents of BM and PM at 4 °C for 6 days.

storage. Additionally, the reduction in the TBARS values might be related to subsequent polymerization, volatilization, or glycation reaction with proteins (Kim, Nam, & Ahn, 2002).

3.2. Analysis of AA contents

AA, the building blocks of proteins, which are often used to evaluate the nutritional value of milk. The AA content in BM and PM during storage were quantified and showed in Tables 1 and 2. It was found that 17 AA in PM were significantly higher than those in BM ($P < 0.05$), in which glutamic acid and proline were particularly significant. Glutamic acid, as one of the most abundant free AA in breast milk, is essential for infants growth and development (Hoang et al., 2025). Proline has also been proven to enhance the stability of peptides derived from milk proteins in the course of gastric digestion (Lopez et al., 2020). Additionally, the levels of lysine, arginine, and leucine in PM were significantly higher than those in BM ($P < 0.05$), and they have the effect of promoting insulin secretion in human body (Muñoz et al., 2026). Among them, lysine, as an important target for protein modification, can affect the protein-protein interactions and the utilization of proteins (Walczak, Schreinert, Gutsche, & Hellwig, 2025). With the storage time progressed, the AA contents in BM increased continuously, while the AA contents in PM increased first and reached a peak at 5d before turning to decrease. This difference was associated to the composition of raw milk. Compared with BM, PM showed significantly higher levels of protein and lipids ($P < 0.05$, Table S2), polyunsaturated fatty acids of PM generated a large amount of reactive carbonyl compounds during oxidation, which further reacted with the nucleophilic groups in proteins (mainly cysteine, lysine, arginine, and histidine residues), promoting the formation of advanced lipid oxidation end products and accelerating AA consumption. Therefore, the AA contents in PM gradually decreased after 5d due to the increase in oxidation reactions, which were intensified in the early storage period, causing AA content to first rise and then fall.

3.3. Analysis of the contents of carbonyl groups

Protein oxidation is a major contributor to the deterioration of dairy product quality. Carbonyl groups represent characteristic products arising from AA oxidation within protein side chains, and their levels directly correlate with the extent of protein oxidation (Zhang et al., 2025). As illustrated in Fig. 2, PM exhibited significantly higher levels of carbonyl groups than BM ($P < 0.05$), suggesting a greater degree of protein oxidation in PM. This difference may be partly attributed to the distinct protein compositions of the two milks (Zhao et al., 2025), as well as to their differential contents of fat and metal ions. First, due to its higher fat content and greater proportion of unsaturated fatty acids, PM was more prone to lipid oxidation (Csapó, Csapó-Kiss, & Házas, 1996), thereby generating reactive carbonyl species that attacked the nucleophilic groups on proteins and consequently accelerated oxidative damage (Milkovska-Stamenova et al., 2017). Second, the concentrations of iron and copper in PM were approximately 2 and 4 times those in BM, respectively (Csapó et al., 1996). Both metal ions are pro-oxidant and can catalyze the Fenton reaction to produce hydroxyl radicals even under refrigerated storage, further accelerating protein oxidation. Notably, in the early stage, the rapid decline of carbonyl groups in PM paralleled a reduction in AA contents (Table 2), implying that newly formed reactive carbonyl species might undergo nucleophilic addition (e.g., Michael addition) with endogenous amino compounds including free AA, thereby decreasing free carbonyl concentrations (Arena et al., 2025; Milkovska-Stamenova et al., 2017).

3.4. Analysis of the contents of sulfhydryl groups

The cysteine residue is the most sensitive AA to oxidative modification in proteins (Stadtman, 1993), and its characterization requires the determination of sulfhydryl group content. In Fig. 3, during 0–4 d, the sulfhydryl group content in BM decreased sharply by 63.84%. In contrast, the initial value of sulfhydryl groups in PM was only 9.60% of that in BM, and it showed a slight fluctuating increase of 28.17%. These results indicated fundamental compositional and structural differences among the proteins in two types of raw milk. The primary source of free sulfhydryl groups in BM was β-lactoglobulin which Cys-121 site are highly prone to oxidation and consumption in early stage of storage (Stadtman, 1993), causing a marked decrease in sulfhydryl levels. In PM, β-lactoglobulin content was low and its structure inherently lacks free sulfhydryl groups (Kessler & Brew, 1970; Koirala et al., 2024; Zhao et al., 2024). Thus, the initial sulfhydryl group level in PM was extremely low and remained stable during storage, with the slight fluctuations observed potentially attributable to conformational changes in other proteins (Ma, Xu, Chen, & Zeng, 2026).

3.5. Analysis of surface hydrophobicity

Surface hydrophobicity is essential for stabilizing tertiary structure

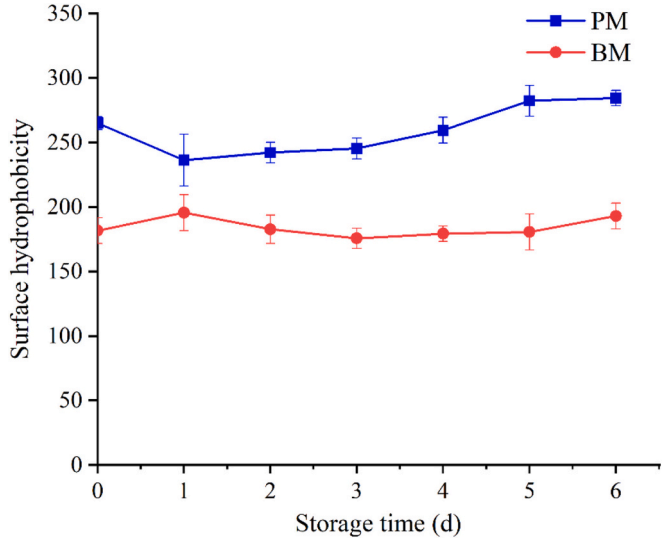


Fig. 4. The changes of H_0 of BM and PM at 4 °C for 6 days.

of proteins, directly affecting their structural stability and functional properties (Han et al., 2020). In Fig. 4, the surface hydrophobicity of both PM and BM samples showed a continuous increase trend throughout the storage period ($P < 0.01$). The oxidation changed protein conformation and led to the exposure of hydrophobic regions embedded within protein during storage (Yan, Ma, et al., 2024), providing more binding sites for ANS probe, and resulting in a significant increase in H_0 (He et al., 2026). Furthermore, lipid oxidation products in PM could form irreversible covalent adducts with proteins, thereby disrupting the native tightly folded conformation of proteins, exposing buried hydrophobic groups, resulting in the H_0 of PM consistently higher than that of BM (Yuan et al., 2019). In summary, lipid oxidation-induced protein denaturation and covalent modification during storage were key factor to the H_0 difference between PM and BM.

3.6. Analysis of the intensities of endogenous fluorescence

Fig. 5 shows that the fluorescence intensities of PM and BM demonstrated an overall increase trend over the course of storage, reflecting that the protein structure became more loose during the oxidation process and exposing more hydrophobic AA residues (Yan, Ma, et al., 2024; Zhang et al., 2024). During storage, the endogenous fluorescence intensities of PM were significantly lower than those of BM ($P < 0.05$), mainly due to the more intense lipid oxidation-protein co-oxidation process in PM. The lipid oxidation in PM could generate active radicals, which readily attack fluorescent AA residues such as tryptophan in milk protein, thereby causing fluorescence quench. Similar results have been reported by (Liao et al., 2026). Although the protein structure of PM expanded more fully due to a higher degree of oxidation, the stronger oxidation quenching effect still caused its overall fluorescence intensities to be lower than that of BM.

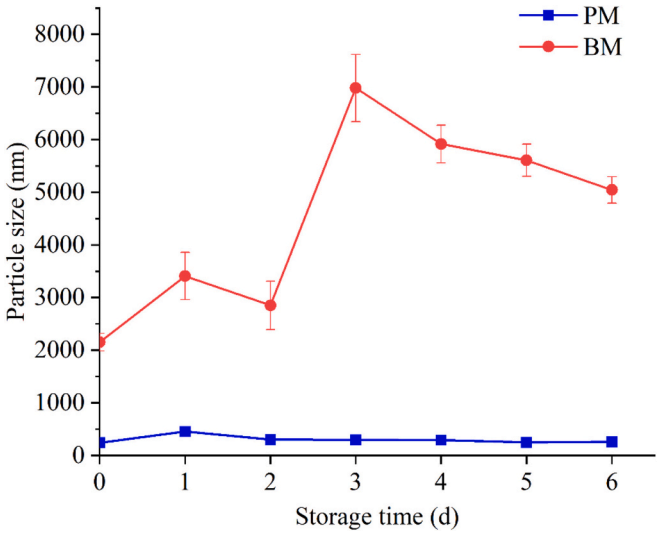


Fig. 6. The changes of particle sizes of BM and PM at 4 °C for 6 days.

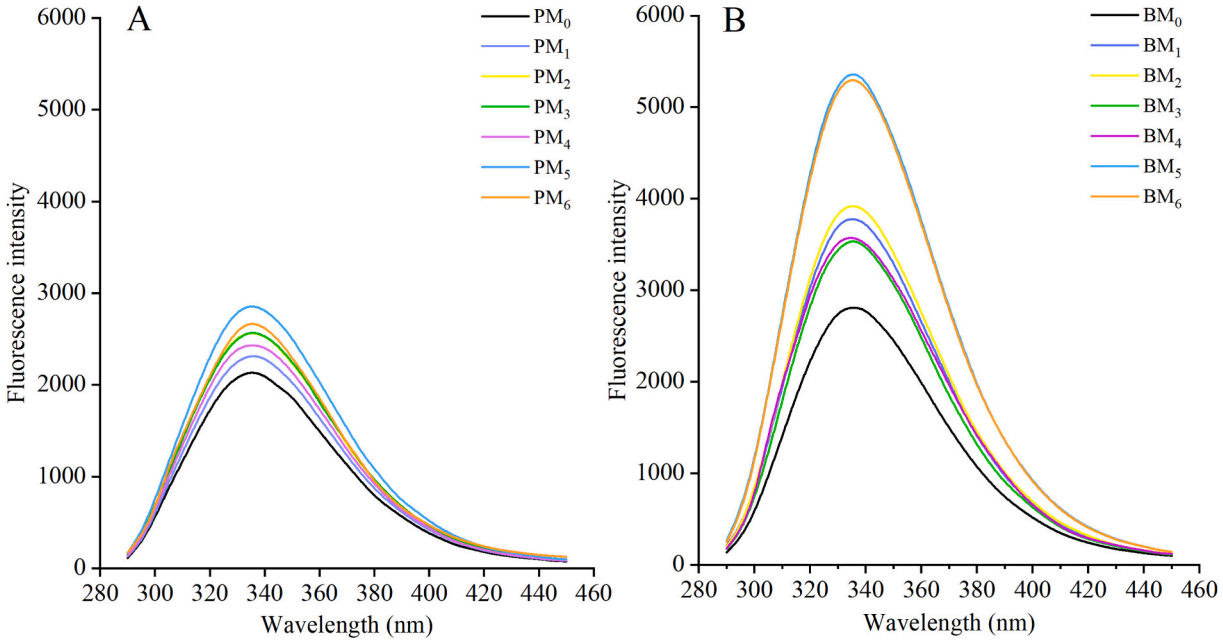


Fig. 5. The intensities of endogenous fluorescence of PM (A) and BM (B) at 4 °C for 6 days.

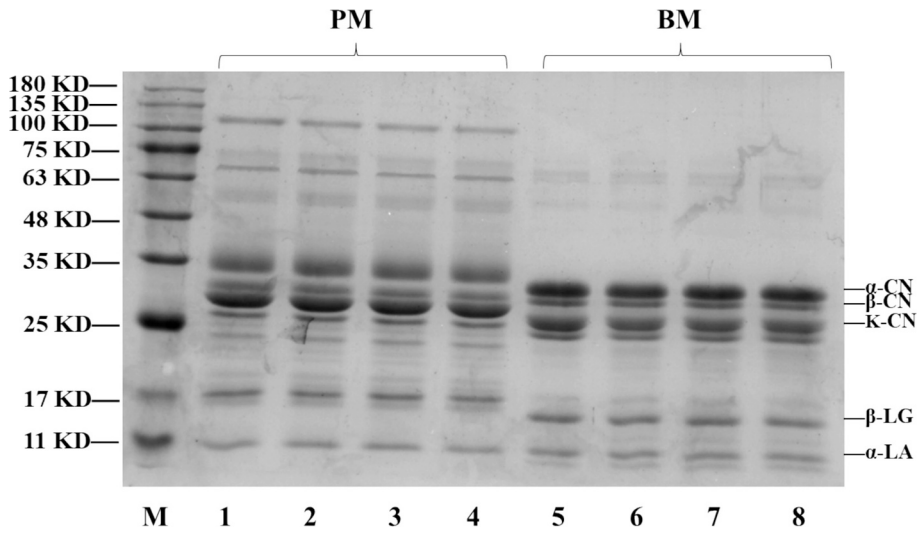


Fig. 7. SDS-PAGE gels of PM and BM (lane 1–4 were PM_0, PM_2, PM_4, PM_6; lane 5–8 were BM_0, BM_2, BM_4, BM_6).

3.7. Analysis of the changes of particle sizes

As storage time increased, the particle sizes of BM increased initially before decreasing, whereas those of PM remained relatively stable (Fig. 6). Compared with PM, the particle size values of BM were significantly higher ($P < 0.01$), which was associated with its higher proportion of colloidal calcium casein (Gallagher, Cotter, & Mulvihill, 1997), a crucial component for regulating micelle assembly and structural stability (Holt, Carver, Ecroyd, & Thorn, 2013). The higher colloidal calcium casein content led to a denser, more rigid micelle network, increasing steric hindrance. Concurrently, the abundant negative charges on the surface of PM micelles could improve the electrostatic environment of the system, strengthening the electrostatic repulsion between micelles and between micelles and fat globules. The synergistic effects of enhanced steric hindrance and electrostatic repulsion in PM indirectly improved fat globule dispersion stability, thus providing stronger resistance to aggregation (Gallagher et al., 1997). These difference in particle sizes influenced nutritional function directly. The smaller fat globules in PM exhibited a greater surface-to-volume ratio, thereby promoting enzymatic accessibility and favoring lipid hydrolysis and absorption (Roy, Ye, Moughan, & Singh, 2020; Singh & Gallier, 2017).

3.8. Analysis of SDS-PAGE

The cross-linking and changes of molecular weight in raw milk could be determined by SDS-PAGE. In Fig. 7, PM samples had clear bands in higher molecular weight (>100 kDa), proving that stable covalent cross-linked high molecular weight polymers have formed in PM. The absence of these bands in BM samples, indicating that a significantly lower degree of covalent cross-linking among its proteins compared to PM under the same storage conditions. This finding was consistent with the higher levels of lipid and protein oxidation measured in PM, proving that the relatively intense oxidative environment was the primary cause of the cross-linking. Furthermore, compared with BM, the casein micelles in PM have smaller particle sizes and higher κ-casein contents. This protein was more prone to non-specific aggregation through hydrophobic interactions, resulting in aggregation bands appearing in high molecular weigh (Dalgleish & Corredig, 2012; Gallagher et al., 1997). Hence, the structural characteristics of high lipid and protein contents in PM jointly fostered a matrix environment that was highly conducive to oxidation and aggregation, and this environment was the major contributor for the formation of high molecular weight protein polymers in PM.

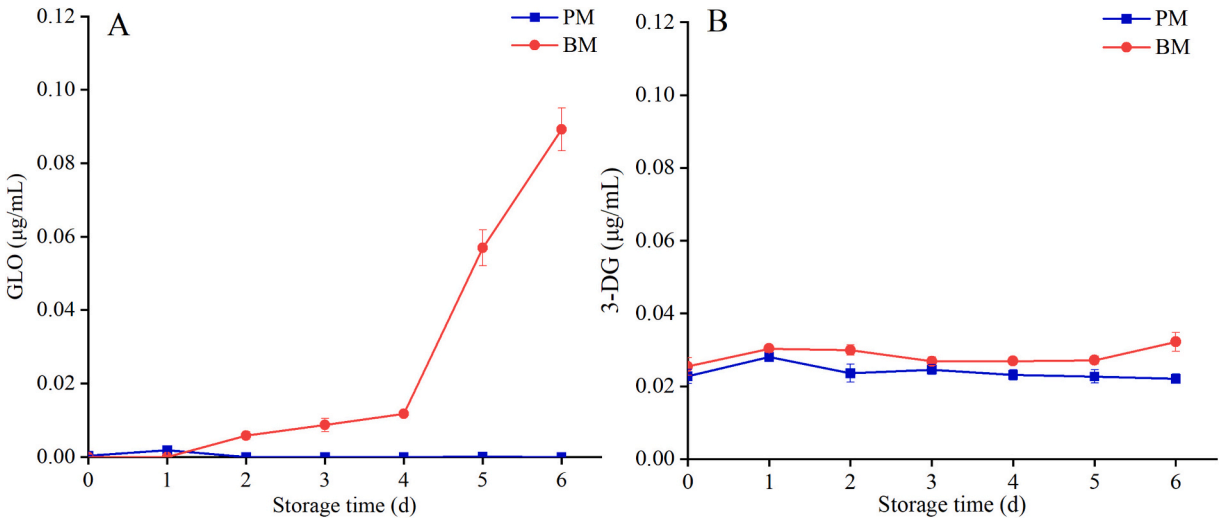


Fig. 8. GLO (A) and 3-DG (B) contents of BM and PM at 4 °C for 6 days.

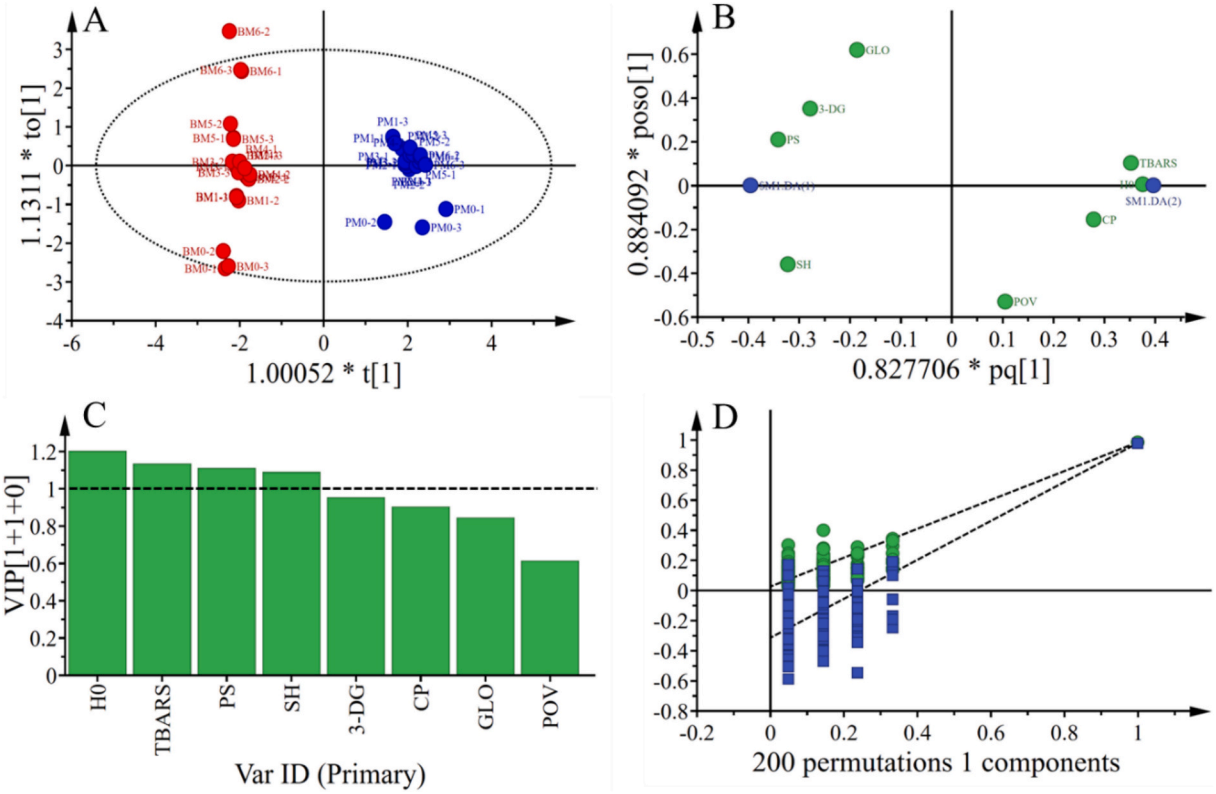


Fig. 9. OPLS-DA results: (A) Score plot, (B) Loading plot, (C) VIP values, and (D) Permutation test plot (200 permutations) carbonyl groups: CP, sulfhydryl groups: SH, particle sizes: PS.

3.9. Analysis of the contents of α-carbonyl compounds

Glyoxal and methylglyoxal were typical dicarbonyl compounds with high reactivity (Yu, Xu, & Yu, 2017). During the experiment, glyoxal and methylglyoxal were not detected, which might be due to their rapid participation in reaction resulting in an insufficient accumulation. GLO and 3-DG were typical six-carbon carbonyl compounds, mainly derived from the oxidation of reducing sugars and glycation reaction (Zhang, Poojary, Olsen, Ray, & Lund, 2019). As shown in Fig. 8, BM exhibited significantly higher levels of generated GLO and 3-DG than PM ($P < 0.01$), with their levels in BM increasing gradually during storage ($P < 0.05$). Notably, the oligosaccharide content in PM was 13.8 times than that in BM (Le Gall, Thoulouze, Richer, Lepvrier, & Le Huërou-Luron, 2025), thus the molecular size and spatial steric hindrance of oligosaccharide were higher than those of lactose, which was not conducive to the occurrence of oxidation and glycation reaction in PM. It has been previously demonstrated that unsaturated fatty acids could inhibit carbohydrate oxidation, and PM contained higher levels of unsaturated fatty acids than BM, thus this inhibition effect was more significant (Zhao et al., 2021). Although unsaturated fatty acids can promote the formation of 3-DG in Maillard reaction, this promoting effect was not manifested due to the large steric hindrance of the glycation reaction in PM (Han et al., 2013; Zhao et al., 2021). Furthermore, since the low temperature (4 °C) hindered the glycation reaction process, and 6-day storage might not be long enough to allow the reaction intermediates to fully transform into detectable AGEs, such as N^{ε}-(carboxymethyl) lysine, N^{ε}-(carboxyethyl)lysine, and pyrraline, thus AGEs were also not detected.

In conclusion, the glycation reaction in raw milk were still in the initial stage. The degree of carbohydrate oxidation and glycation reaction in BM was higher than that in PM, indicating that the dominant reaction pathways were different for two types of raw milks during refrigerated storage. BM tended to be dominated by carbohydrate oxidation and glycation reaction, while PM was more inclined to be dominated by lipid oxidation and protein oxidation.

3.10. Comparison of oxdation indicators in BM and PM by OPLS-DA

An OPLS-DA model was employed to discriminate between BM and PM (Fig. 9A). Fitted parameters of this model, R^2X_{cum}, R^2Y_{cum}, and Q^2_{cum} values were 0.723, 0.985, and 0.980, suggesting goodness of fit. Consistent with the loading plot (Fig. 9A), the eigenvector values (Fig. 9B) showed that H_0 (eigenvector, +0.375329) had a positive sign while particle size (eigenvector, −0.340795) had a negative sign, indicating that H_0 was associated with the PM side of the discriminant component, and particle size with the BM side. Furthermore, variable important in projection (VIP) values>1 indicated that the product were significant for discrimination. The H_0, TBARS, particle size, and sulfhydryl groups (VIP values: 1.20477, 1.13696, 1.11276, 1.09142), were identified as key indicators to distinguish BM and PM (Fig. 9C). To avoid overfitting and ensure the reliability of the OPLS-DA model, an external validation test (permutation test) was required. The R^2Y (0.00263) and Q^2Y (−0.314) values obtained from 200 permutation tests were < 0.1 (Fig. 9D), ensuring that the model does not overfit. Therefore, the model obtained in this experiment was reliable.

Based on the key indicators H_0, particle sizes, TBARS and sulfhydryl groups obtained from OPLS-DA, we found that the high H_0 values of PM were consistent with its high molecular weight aggregation in SDS-PAGE, suggested that it has undergone protein aggregation mainly through hydrophobic interactions. The particle sizes of PM remained stable during storage, which was associated with the formation of large spatial steric hindrance and electrostatic repulsion of its casein micelles (de Kruif, Huppertz, Urban, & Petukhov, 2012; Du et al., 2023); while the fluctuation of the particle sizes of BM was related to the dominant modification of carbohydrate oxidation and glycation reaction. At the same time, the higher TBARS values and lower sulfhydryl groups of PM

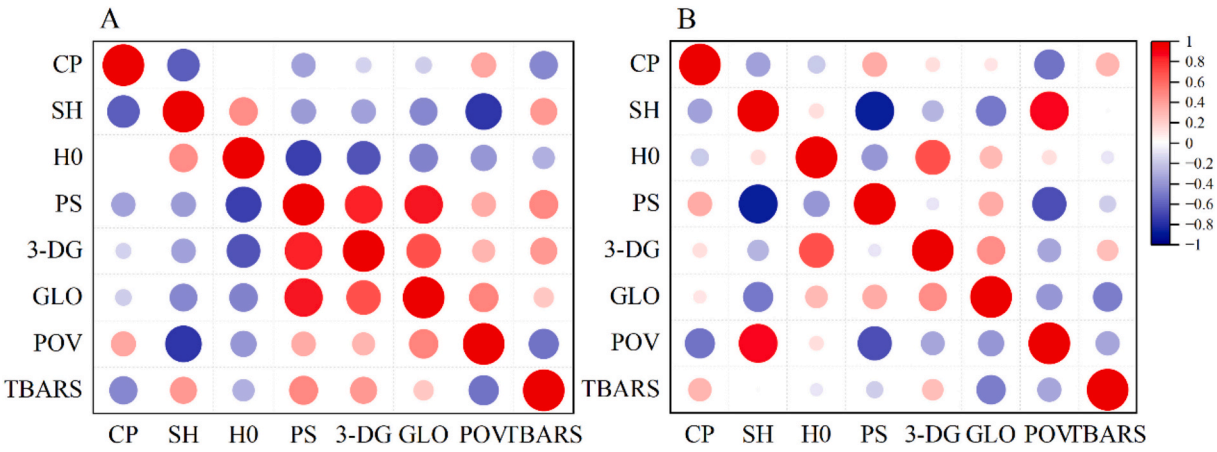


Fig. 10. Correlation heatmap of PM (A) and BM (B) carbonyl groups: CP, sulfhydryl groups: SH, particle sizes: PS.

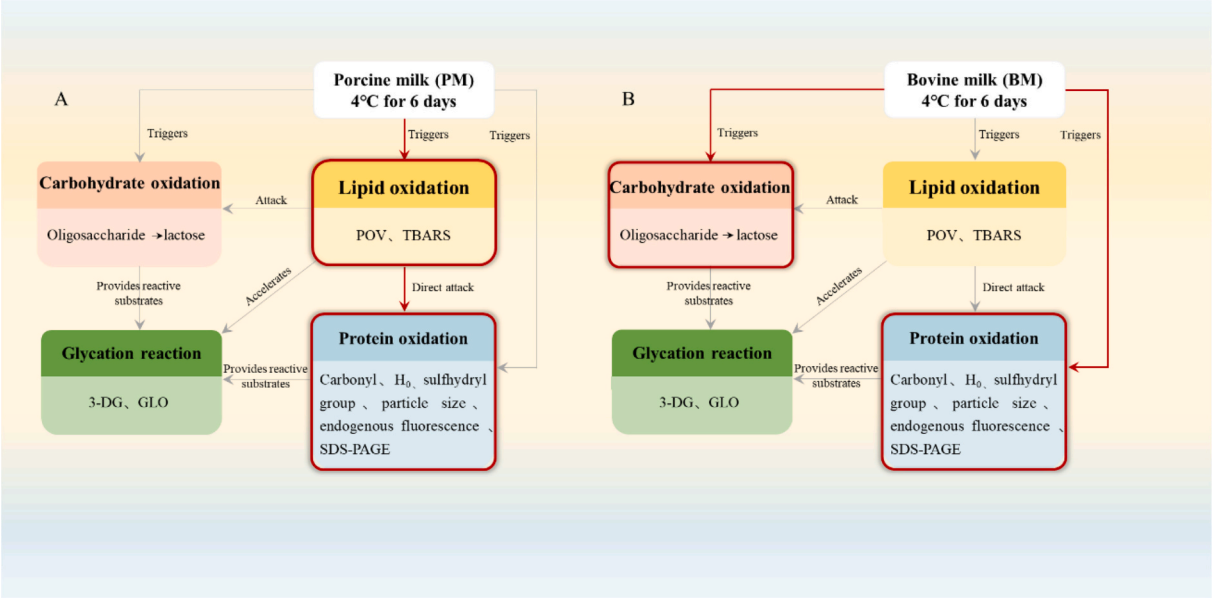


Fig. 11. Possible oxidation pathway of the main components in PM (A) and BM (B).

further confirmed that the lipid oxidation and protein oxidation of PM were more intense. These results systematically indicated that PM and BM exhibited different dominant oxidative pathways and structural change patterns under the same storage conditions.

3.11. *Correlation analysis between oxidation indicators*

The correlation between oxidation indicators in PM or BM was further investigated separately. Notably, distinct correlation patterns emerged in PM and BM (Fig. 10). In PM, lipid oxidation was more closely related to protein structure changes. Specifically, TBARS values significantly correlated with particle sizes, carbonyl groups and sulfhydryl groups (Fig. 10A). This result further confirmed that the accumulation of carbonyl groups in PM was closely related to its lipid oxidation process. Considering the high content of unsaturated fatty acids in PM, we hypothesized that these unsaturated fatty acids could drive protein oxidation and glycation reaction via lipid oxidation pathways during storage (Fig. 11A).

In contrast, there was a trend of concurrent enhancement between protein structure change and glycation process in BM. Specifically, the H_0 values showed a significant positive correlation with 3-DG and GLO contents (Fig. 10B), demonstrating that during the storage of BM, the glycation reaction promoted the unfolding of protein side chains, which exposed more hydrophobic groups and consequently increased the protein's surface hydrophobicity. Meanwhile, the POV values in BM were significantly negatively correlated with particle sizes and strongly positively correlated with sulfhydryl group contents (Fig. 10B). This indicated that lipid oxidation did not directly cause significant protein oxidation damage (such as carbonylation or loss of sulfhydryl groups), but was related to the change in protein aggregation state. It suggested that lipid oxidation might indirectly regulate the process and product accumulation of glycation reaction by promoting protein dispersion and exposing some sulfhydryl groups. This result was also consistent with the significant contribution of particle sizes and sulfhydryl groups contents to model discrimination in OPLS-DA (Fig. 9B and Fig. 9C).

Thus, it could be seen that the key indicators revealed by correlation analysis in BM and PM were highly overlapping with the key factors with VIP $>$ 1 in OPLS-DA, indicating that the two statistical methods have verified the key roles of H_0, TBARS, particle sizes, and sulfhydryl groups in reflecting the oxidation and glycation processes of the milk system from different perspectives.

4. Conclusion

This study systematically investigated the dynamic processes of protein oxidation, lipid oxidation and glycation reaction in PM and BM from commercial farms during storage, and identified the differences in the dominant oxidation pathways between two types of raw milk. The levels of primary and secondary lipid oxidation products, carbonyl group contents, surface hydrophobicity and high-molecular aggregation degree of PM were significantly higher than those of BM, while BM had significantly higher levels of sulfhydryl group contents, endogenous fluorescence intensities, 3-DG and GLO contents, and its particle sizes first increased and then fluctuated downward. These results demonstrated differences in oxidation states of the two types of raw milk during storage. The OPLS-DA model further identified these differences might be related to surface hydrophobicity, TBARS, particle sizes, and sulfhydryl groups. Correlation analysis revealed that the TBARS values in PM exhibited significant correlation with the levels of particle size, carbonyl groups, and sulfhydryl groups ($P < 0.05$). In BM, the H_0 values were significantly positively correlated with 3-DG and GLO contents ($P < 0.05$). These findings further indicated that the oxidation pathways of BM and PM were significantly different during storage. Specifically, PM was dominated by lipid oxidation, presented as the co-oxidation of protein and lipids; while BM was related to carbohydrate oxidation and glycation reactions, showing a synergistic increase in protein structure changes and glycation intermediate product accumulation. In addition, the higher AA contents and smaller fat globule particle sizes in PM suggested that it had certain advantages in terms of nutritional retention and digestive characteristics. This study characterizes the oxidation pathways and interaction patterns of PM and BM under refrigerated storage, and explores the potential mechanisms underlying their differential behaviors, providing a reference for the storage stability and further utilization of different milk sources in dairy products.

CRediT authorship contribution statement

Qiao Jiang: Writing – original draft, Data curation, Conceptualization. **Haixia Yan:** Writing – original draft, Data curation, Conceptualization. **Mo Li:** Validation, Software, Methodology. **Li Zhou:** Visualization, Formal analysis. **Jie Wu:** Writing – review & editing, Supervision, Resources. **Xin Zhao:** Writing – review & editing, Project administration, Funding acquisition.

Declaration of competing interest

The authors declare that they have no known competing financial interests or personal relationships that could have appeared to influence the work reported in this paper.

Acknowledgements

Financial support from PhD Start-up Foundation of Liaoning Province (2023-BSBA-301, 2025-BS-0260), the Science and Technology Research Project of the Department of Education of Liaoning Province (LJ212510164011), China Adult Education Association's 2025-2026 Research Project on “Artificial Intelligence+Lifelong Learning” (Y2025184S), Liaoning Provincial Key Research and Development Program (Nos. 2024JH2/102500079), Shenyang City Special Project for the Cultivation of Young and Middle-aged Scientific and Technological Innovation Talents (RC240110) is gratefully acknowledged.

Appendix A. Supplementary data

Supplementary data to this article can be found online at https://doi.org/10.1016/j.fochx.2026.104405.

Data availability

Data will be made available on request.

References

Akıllıoğlu, H. G., Chatterton, D. E. W., & Lund, M. N. (2022). Maillard reaction products and amino acid cross-links in liquid infant formula: Effects of UHT treatment and storage. *Food Chemistry, 396*, Article 133687. https://doi.org/10.1016/j.foodchem.2022.133687

Arena, S., De Pascale, S., Ciaravolo, V., Monroy, M. M., Gouw, J. W., Stahl, B., … Troise, A. D. (2025). Protein-bound and free glycation compounds in human milk: A comparative study with minimally processed infant formula and pasteurized bovine milk. *Food Chemistry, 463*, Article 141265. https://doi.org/10.1016/j.foodchem.2024.141265

Csapó, J., Martin, T. G., Csapó-Kiss, Z. S., & Házas, Z. (1996). Protein, fats, vitamin and mineral concentrations in porcine colostrum and milk from parturition to 60 days. *International Dairy Journal, 6*, 881–902.

Dalgleish, D. G., & Corredig, M. (2012). The structure of the casein micelle of Milk and its changes during processing. *Annual Review of Food Science and Technology, 3*(1), 449–467. https://doi.org/10.1146/annurev-food-022811-101214

Dong, L., Li, Y., Chen, Q., Liu, Y., Qiao, Z., Sang, S., Zhang, J., Zhan, S., Wu, Z., & Liu, L. (2023). Research advances of advanced glycation end products in milk and dairy products: Formation, determination, control strategy and immunometabolism via gut microbiota. *Food Chemistry, 417*, Article 135861. https://doi.org/10.1016/j.foodchem.2023.135861

Du, Z., Xu, N., Yang, Y., Li, G., Tai, Z., Li, N., & Sun, Y. (2023). Study on internal structure of casein micelles in reconstituted skim milk powder. *International Journal of Biological Macromolecules, 224*, 437–452. https://doi.org/10.1016/j.ijbiomac.2022.10.135

Fernandez-Avila, C., Gutierrez-Merida, C., & Trujillo, A. J. (2017). Physicochemical and sensory characteristics of a UHT milk-based product enriched with conjugated linoleic acid emulsified by ultra-high pressure homogenization. *Innovative Food Science & Emerging Technologies, 39*, 275–283. https://doi.org/10.1016/j.ifset.2017.01.001

Gallagher, D. P., Cotter, P. F., & Mulvihill, D. M. (1997). Porcine Milk proteins: A review. *International Dairy Journal*, 99–118.

Han, L., Li, L., Li, B., Zhao, D., Li, Y., Xu, Z., & Liu, G. (2013). Glyoxal derived from triglyceride participating in diet-derived Nε-carboxymethyllysine formation. *Food Research International, 51*(2), 836–840. https://doi.org/10.1016/j.foodres.2013.01.051

Han, T., Wang, M., Wang, Y., & Tang, L. (2020). Effects of high-pressure homogenization and ultrasonic treatment on the structure and characteristics of casein. *LWT- Food Science and Technology, 130*, Article 109560. https://doi.org/10.1016/j.lwt.2020.109560

He, J., Wang, D., Wang, T., & Ji, R. (2026). Effects of heat treatment on camel milk physicochemical properties, microstructure and protein profiling. *LWT–Food Science and Technology, 239*, Article 118800. https://doi.org/10.1016/j.lwt.2025.118800

Hoang, K. H. T., Nguyen, M. T. T., An, Y., Jung, J. A., Israr, B., & Kim, J. (2025). Distribution of free amino acids in human breast milk from Asian countries. *Journal of Food Composition and Analysis, 148*, Article 108185. https://doi.org/10.1016/j.jfca.2025.108185

Holt, C., Carver, J. A., Ecroyd, H., & Thorn, D. C. (2013). Invited review: Caseins and the casein micelle: Their biological functions, structures, and behavior in foods. *Journal of Dairy Science, 96*(10), 6127–6146. https://doi.org/10.3168/jds.2013-6831

Ji, Z., Meng, L., Sun, X., Han, R., Yang, Y., Wang, J., & Zheng, N. (2025). Comprehensive analysis of species-specific differences in fatty acid composition and proteome of milk fat globules in human and animals. *Food Chemistry: X, 27*, Article 102431. https://doi.org/10.1016/j.fochx.2025.102431

Jin, S., Liao, J., Sun, Y., Wang, R., Li, L., Wu, L., Wei, J., Wang, P., Ren, F., & Wang, Y. (2026). Size-dependent lipidomics and fatty acid profiles of fat globules in buffalo milk. *Food Chemistry, 517*, Article 149481. https://doi.org/10.1016/j.foodchem.2026.149481

Kessler, E., & Brew, K. (1970). The whey proteins of pig's milk. Isolation and characterization of a beta-lactoglobulin. *Biochimica et Biophysica Acta, 200*, 449–458. https://doi.org/10.1016/0005-2795(70)90101-7

Kim, Y. H., Nam, K. C., & Ahn, D. U. (2002). Volatile profiles, lipid oxidation and sensory characteristics of irradiated meat from different animal species. *Meat Science, 61*(3), 257–265. https://doi.org/10.1016/S0309-1740(01)00191-7

Koirala, P., Malav, O. P., Rai, S., Palanisamy, G., Agrawal, A., Dhar, B. K., … Nirmal, N. (2024). Impact of non-bovine milks and milk products on human gut microbiota: A perspective towards sustainable healthy food production. *Trends in Food Science & Technology, 151*, Article 104642. https://doi.org/10.1016/j.tifs.2024.104642

de Kruif, C. G., Huppertz, T., Urban, V. S., & Petukhov, A. V. (2012). Casein micelles and their internal structure. *Advances in Colloid and Interface Science, 171-172*, 36–52. https://doi.org/10.1016/j.cis.2012.01.002

Le Gall, S., Thoulouze, L., Richer, Y., Lepvrier, E., & Le Huërou-Luron, I. (2025). Exploring animals and human milk oligosaccharides: A comprehensive analysis using hydrophilic interaction liquid chromatography coupled with fluorescent and mass spectrometry detectors. *Journal of Food Composition and Analysis, 147*, Article 108074. https://doi.org/10.1016/j.jfca.2025.108074

Li, H., Xi, B., Yang, X., Wang, H., He, X., Li, W., & Gao, Y. (2022). Evaluation of change in quality indices and volatile flavor components in raw milk during refrigerated

storage. *LWT- Food Science and Technology, 165*, Article 113674. https://doi.org/10.1016/j.lwt.2022.113674

Liao, Y., Ma, L., Gao, Y., Pei, Y., Qi, B., & Li, Y. (2026). The role of interfacial protein composition in the stability of soybean oil bodies: Elucidating the mechanism of protein-lipid co-oxidation under different extraction conditions. *Food Research International, 223*, Article 117893. https://doi.org/10.1016/j.foodres.2025.117893

Lopez, C., Adelfio, A., Wall, A. M., Molloy, B., Holton, T. A., & Khaldi, N. (2020). Human milk and infant formulae: Peptide differences and the opportunity to address the functional gap. *Current Research in Food Science, 3*, 217–226. https://doi.org/10.1016/j.crfs.2020.07.003

Ma, Q., Xu, Q., Chen, N., & Zeng, W. (2026). Regulation of disulfide bond cleavage on the physicochemical and digestive properties of EGCG-gluten covalent complexes. *Food Hydrocolloids, 170*, Article 111724. https://doi.org/10.1016/j.foodhyd.2025.111724

Malacarne, M., Summer, A., Franceschi, P., Formaggioni, P., Pecorari, M., Panari, G., Vecchia, P., Sandri, S., Fossa, E., Scotti, C., & Mariani, P. (2013). Effects of storage conditions on physico-chemical characteristics, salt equilibria, processing properties and microbial development of raw milk. *International Dairy Journal, 29*(1), 36–41. https://doi.org/10.1016/j.idairyj.2012.10.005

Meucci, V., Lenzi, A., Armani, A., Pedonese, F., Ghimenti, L., & De Marchi, L. (2025). Assessing ochratoxin a contamination in pre-packaged grated cheese: Implications for food safety. *Foods, 14*(9), Article 1504. https://doi.org/10.3390/foods14091504

Milkovska-Stamenova, S., Mnatsakanyan, R., & Hoffmann, R. (2017). Protein carbonylation sites in bovine raw milk and processed milk products. *Food Chemistry, 229*, 417–424. https://doi.org/10.1016/j.foodchem.2017.02.102

Mitina, A., Mazin, P., Vanyushkina, A., Anikanov, N., Mair, W., Guo, S., & Khaitovich, P. (2020). Lipidome analysis of milk composition in humans, monkeys, bovids, and pigs. *BMC Evolutionary Biology, 20*(1), 70. https://doi.org/10.1186/s12862-020-01637-0

Muñoz, F., Gao, Q., Mattanovich, M., Trost, K., Hodek, O., Lindqvist, A., … Cataldo, L. R. (2026). Lysine potentiates insulin secretion via AASS-dependent catabolism and regulation of GABA content and signaling. *Metabolism, 174*, Article 156423. https://doi.org/10.1016/j.metabol.2025.156423

Pont, E. G. (1952). Studies on the origin of oxidized flavour in whole milk. *Journal of Dairy Research, 19*(3), 316–327.

Qin, C., Liu, L., Wang, Y., Leng, T., Zhu, M., Gan, B., Xie, J., Yu, Q., & Chen, Y. (2022). Advancement of omics techniques for chemical profile analysis and authentication of milk. *Trends in Food Science & Technology, 127*, 114–128. https://doi.org/10.1016/j.tifs.2022.06.001

Ratel, J., Vigneau, E., Mercier, F., Lebreton, S., Nguyen, T. L. N., Courcoux, P., & Engel, E. (2024). Implementation of sample pooling to strengthen the surveillance of food chemical safety: Case study of nDL-PCBs in pork meat. *Food Chemistry, 433*, Article 137111. https://doi.org/10.1016/j.foodchem.2023.137111

Roy, D., Ye, A., Moughan, P. J., & Singh, H. (2020). Composition, structure, and digestive dynamics of milk from different species-a review. *Food & Function, 7*, Article 577759. https://doi.org/10.3389/fnut.2020.577759

Singh, H., & Gallier, S. (2017). Nature's complex emulsion: The fat globules of milk. *Food Hydrocolloids, 68*, 81–89. https://doi.org/10.1016/j.foodhyd.2016.10.011

Stadtman, E. R. (1993). Oxidation of free amino acids and amino acid residues in proteins by radiolysis and by metal-catalyzed reactions. *Annual Review of Biochemistry, 62*, 797–821. https://doi.org/10.1146/annurev.bi.62.070193.004053

Walczak, M., Schreinert, S., Gutsche, F., & Hellwig, M. (2025). N-ε-methylated lysine derivatives in food. *Journal of Food Composition and Analysis, 148*, Article 108633. https://doi.org/10.1016/j.jfca.2025.108633

Wu, Y., Sun, Y., Chen, R., Qiao, Y., Zhang, Q., Li, Q., Wang, X., Pan, Y., Li, S., & Wang, Z. (2023). Analysis for lipid nutrient differences in the milk of 13 species from a quantitative non-targeted lipidomics perspective. *Food Chemistry: X, 20*, Article 101024. https://doi.org/10.1016/j.fochx.2023.101024

Yan, H., Huang, W., Zhao, X., Ge, C., Shen, Y., & Liu, L. (2024). Effect of fatty acid composition on the volatile compounds of pasteurized milk during low-temperature storage. *Food Research International, 195*, Article 114990. https://doi.org/10.1016/j.foodres.2024.114990

Yan, H., Ma, C., Shen, Y., Ye, B., & Liu, L. (2024). Effect of lipid-mediated moisture status on casein characteristic in two types of milk powders during accelerated storage. *eFood, 5*(4), Article 145289. https://doi.org/10.1002/efd2.168

Ye, Y., Engholm-Keller, K., Fang, Y., Nielsen, C. F., Jordà, A., Lund, M. N., & Chatterton, D. E. W. (2022). UHT treatment and storage of liquid infant formula affects protein digestion and release of bioactive peptides. *Food & Function, 13*(1), 344–355.

Yu, P., Xu, X. B., & Yu, S. J. (2017). The effect of pH and amino acids on the formation of methylglyoxal in a glucose–amino acid model system. *Journal of the Science of Food and Agriculture, 97*(10), 3159–3165. https://doi.org/10.1002/jsfa.8158

Yuan, Y., Pan, B., Niu, X., Yao, X., Sun, M., Xu, M., & Zhu, Q. (2019). Impacts of epicatechin on the formation of advanced lipid oxidation end products (ALEs) in a fish oil oxidation model. *LWT- Food Science and Technology, 111*, 582–587. https://doi.org/10.1016/j.lwt.2019.05.081

Zhang, H., Abdallah, M. F., Zhang, J., Yu, Y., Zhao, Q., Tang, C., … Zhang, J. (2022). Comprehensive quantitation of multi-signature peptides originating from casein for the discrimination of milk from eight different animal species using LC-HRMS with stable isotope labeled peptides. *Food Chemistry, 390*, Article 133126. https://doi.org/10.1016/j.foodchem.2022.133126

Zhang, T., Liu, Y., Cao, J., Jiang, L., Liu, T., & Yi, H. (2024). Experimental and molecular dynamics simulation study on the mechanism of β-lactoglobulin self-aggregation induced by ultra-high temperature. *LWT- Food Science and Technology, 209*, Article 116782. https://doi.org/10.1016/j.lwt.2024.116782

Zhang, W., Poojary, M. M., Olsen, K., Ray, C. A., & Lund, M. N. (2019). Formation of α-Dicarbonyls from dairy related carbohydrates with and without nα-acetyl-l-lysine during incubation at 40 and 50°C. *Journal of Agricultural and Food Chemistry, 67*(22), 6350–6358. https://doi.org/10.1021/acs.jafc.9b01532

Zhang, Z., Zhu, Y., Cheng, W., Hu, M., Yao, X., Yin, Z., & Liu, D. (2025). Regulatory effects of sweet potato pericarp polyphenols on protein oxidation in commercial fresh milk. *Journal of Dairy Science, 108*(12), 13071–13084. https://doi.org/10.3168/jds.2025-27049

Zhao, H., Cao, X., Quan, Z., Liu, X., & Yue, X. (2025). Novel insights into differences in the whey proteome of porcine and human colostrum and mature milk. *Food Chemistry, 478*, Article 143584. https://doi.org/10.1016/j.foodchem.2025.143584

Zhao, H., Zhao, S., Zhu, Q., Chen, J., Quan, Z., Yue, X., & Cao, X. (2024). Label-free-based proteomic analysis reveals differential whey proteins of porcine milk during lactation. *Food Chemistry: X, 21*, Article 101112. https://doi.org/10.1016/j.fochx.2023.101112

Zhao, X., Zhang, X., Ye, B., Yan, H., Zhao, Y., & Liu, L. (2021). Effect of unsaturated fatty acids on glycation product formation pathways. *Food Research International, 143*, Article 110288. https://doi.org/10.1016/j.foodres.2021.110288